Modeling Wind Turbine Interaction: Large Eddy Simulations for the Verification of Empirical Wind Turbine Wake Models

Valentin Bernard
valenin.bernard@tecnico.ulisboa.pt

Instituto Superior Técnico, Lisboa, Portugal

November 2019

Abstract

Wind turbine manufacturers are delivering turbines of ever larger rotor diameter. Predicting fatigue damage and power production requires improved aerodynamic models. Turbine wakes can have a substantial impact on these results, but the phenomenon is still not well understood. The dynamic wake meandering (DWM), recently added to the IEC64100 standard for wind turbines, promises improved load predictions for wind turbines in farm configurations. In this thesis, the implementation of a DWM-based aero-dynamic farm modeling tool is presented in detail. The tool is validated for a turbine impacted by a single wake and verified by comparison with an LES benchmark solution. Limited conclusions are drawn from the verification. Furthermore, a new formulation for wake steering is derived, that is coherent with the overall assumptions of the tool and can be integrated into the tool with ease. Results of the novel formulation are compared to models from literature and LES simulations, finding fair performance.

1. Introduction

The offshore wind energy sector has experienced rapid growth in recent years, and technological progress is strikingly showcased by the 5-fold increase in blade length since the deployment of the first offshore wind farm in 1991 [1]. For new turbines and farms to be reliable and therefore bankable, accurate models for energy yield, resistance to extreme wind conditions and fatigue lifetime are fundamental. The present work focuses specifically on the aerodynamic simulation of *wake effects*. The wake denotes the wind field perturbation downstream of a turbine, where wind speed is reduced and turbulence is increased. Turbines affected by wakes produce less energy and are subject to higher fatigue loads, making accurate wake models essential. In the present work, the state-of-the-art in wake modeling is recapitulated before describing the implementation and validation of an advanced wake modeling tool based on the dynamic wake meandering (DWM) model by DTU [20]. The use of LES benchmarks solutions for verification of the tool is explored. Lastly, a new formulation for wake steering is derived and validated, final conclusions are drawn and future work is laid out.

2. Background on Aerodynamic Modeling for Wakes

For better understanding of the work carried out in this thesis, some general background on wind turbine modeling, wake modeling and CFD for wind turbines is provided.

2.1. Aerodynamic modeling of wind turbines

Before being able to understand wake effects, it is necessary to be able to model the behavior of a wind turbine for any given inflow conditions. Industry standard is to use solvers based on the Blade Element Momentum Theory (BEM), but approaches based on vorticity exist as well (see E. Branlard, 2017 [9]). BEM combines momentum theory and blade element theory obtaining a set of equations that is solved iteratively to obtain the local induction, torque, thrust at a given blade element [23]. Theoretically, the applicability of BEM is limited due to strong assumptions, however corrections have been introduced throughout the years in order to overcome these limitations. Modern BEM-based turbine simulators [2, 27] are able to deal with most aerodynamic effects observed on a single turbine. These simulators generally couple BEM with structural models, models for the control system and even hydrodynamic models for offshore turbines, resulting in so-called 'aero-servo-elastic' solvers. While very adapt at predicting tur-

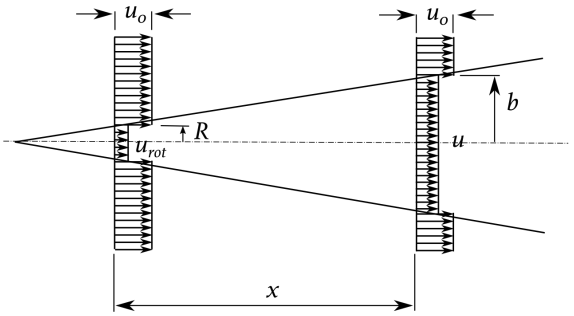

Figure 1: Schematic representation of the Jensen wake model [16].

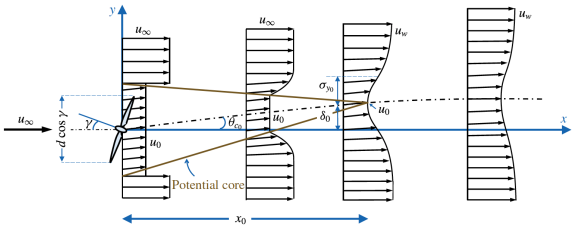

Figure 2: Mass flows, velocities and potential core in the EPFL wake deflection model. After the potential core disappears, the deflection angle and deficit shape become Gaussian [7].

bine behaviour or given inflow conditions, these solvers generally do not consider the effects of surrounding turbines in a farm, notably the presence of wakes. In order to predict the impact of wakes on loads and power at individual turbines, external models are used to generate inflow conditions for the aero-servo-elastic solver.

2.2. Wake effects

The wake of a wind turbine is defined as the disturbance in the atmospheric flow caused by the presence of the turbine. It is generally characterized by reduced wind speed and increased wind fluctuations, *i.e.* turbulence, impacting therefore both energy yield and fatigue lifetime of turbines. In literature, the two effects, wake deficit and added turbulence, are generally modelled separately[16, 19, 6, 11], but wholistic approaches exist [20, 21].

Among the most classical wake deficit models is the model proposed by Jensen [16] that is based on a one-dimensional stream tube where the turbine is modeled by its global thrust coefficient C_T, and only mass conservation is imposed. The model is schematically shown in figure 1 ad is commonly formulated as:

$$\frac{\Delta u}{u_0} = \left(1 - \sqrt{1 - C_T)}\right) / \left(1 + \frac{2k_e x}{D}\right)^2. \qquad (1)$$

where x is the downstream distance and k_e is the linear expansion coefficient of the wake, usually denoted entrainment constant. While simplistic, the Jensen formulation remains widely used and has been repeatedly validated with measurements [13]. It is however unsuitable for generating inflow for aero-servo-elastic solvers due to the non-physical wake field with sharp gradients. The model is only used to obtain an average reduced velocity at a target turbine, from which energy yield is estimated though the power curve.

In order to overcome the sharp gradients in the Jensen model, other literature assumes a Gaussian shape for the deficit [6, 26, 7]. In the model proposed at École Polytechnique Fédérale de Lausanne (EPFL) [7], researchers impose both mass and momentum conservation to model the propagation of a Gaussian velocity deficit far from the turbine, while a *potential core* approach is proposed for the immediate near wake. The authors furthermore adapt the model to allow for the treatment of yawed turbines, were deflected wakes are observed. A schematic representation of the model for a yawed turbine is shown in figure 2, while the final expression, fitted to LES data through 4 parameters, can be found in [7]. The flow field in the wake resulting from the use of a Gaussian model is relatively smooth, and could potentially be used as an inflow field to simulate a wake impacts on a turbine. Additional models for added turbulence would however be necessary.

A more physical approach to wake deficit modeling was proposed by Ainslie [4]. This approach is based on the rotationally symmetric thin-shear-layer approximation of the Navier-Stokes equations, using an eddy-viscosity ν_e to model turbulence. Furthermore, the pressure term is neglected under the limitation that the model is only valid from a few diameters downstream from the rotor, where the pressure has recovered and the wake is fully turbulent. The proposed set of equations reads as follows [20]:

$$\frac{\partial U}{\partial x} + \frac{1}{r}\frac{\partial}{\partial r}(rV) = 0 \qquad (2a)$$

$$U\frac{\partial U}{\partial x} + V\frac{\partial U}{\partial r} = \frac{\nu_e}{r}\frac{\partial}{\partial r}\left(r\frac{\partial U}{\partial r}\right) \qquad (2b)$$

where U and V describe the axial and radial velocities while x and r describe the axial and radial coordinates, centred at the rotor hub. An analytical approximations for the value of ν_e based on characteristic length and velocity scales of the wake is proposed [3]. Numerical methods to solve the equation system. Variations of the Ainslie model have been proposed in literature [20, 21], improving the approximation of the eddy viscosity as well as the boundary conditions.

Ainslie noted that, on order for the model to deliver accurate predict the average velocity on the

impacted rotor, an additional phenomenon must be considred: *wake meandering* [4]. This phenomenon consists in a random, large-scale motion of the entire wake relative to a fixed observer, believed to be caused by fluctuations in the mean wind direction [4] and large-scale turbulence [22]. Ainslie proposes a statistical treatment of the phenomenon, which is sufficient for power estimates but does not contribute to understanding the impact of wake meandering on loads. Again the use of the deficit model in an aero-servo elastic solver is possible due to the smooth wake shape, but a turbulence model is needed.

Generally, added turbulence model try to estimate a value I_+ such that the total turbulence intensity can be derived by linear superposition of the I_+ with the ambient turbulence I_{amb}:

$$I_{wake} = \sqrt{I_0^2 + I_+^2} \tag{3}$$

The most used formulation of this kind is Frandsen's model [12], that also is recommended in the IEC6400 standard for wind turbines [15].

2.3. DWM

The dynamic wake meandering model (DWM) by DTU represents a different approach the treatment of wake than the models mentioned so far [20, 21]. Rather than treating wake deficit and added turbulence separately with different models, a single modeling framework is proposed for all wake phenomena. In the DWM approach, the meandering phenomenon treated dynamically, causing wind speed fluctuations over time and therefore adding turbulence to the wake field. In addition, a simple model for turbulence generated by sheer and the decay of tip vortexes is proposed. This second kind of turbulence is of a smaller scale, and is expected to follow the meandering motion of the wake. The meandering is computed based on the assumption that a turbine emits a stream of *wake particles*, that are convected in axial direction at ambient wind speed and slowly move in lateral and vertical direction. The off-axis velocity of each *particle* is constant and determined at the time of emission from turbulence data. The wake deficit is modeled using an Ainslie approach with refined boundary conditions. 3 sub-models are therefore considered in the DWM approach, wake deficit, wake meandering and small scale added turbulence. The DWM approach was recently added to the IEC61400 standard for wind turbines [15], but has not yet been fully adopted by the industry. The approach can be used to generate inflow for simulations of a wake-impacted turbine without requiring any additional models, making it potentially very useful.

2.4. CFD for wind turbines

Computational fluid dynamics (CFD) denotes a branch of fluid mechanics that uses numerical methods to solve the differential equations that govern fluid flow, commonly known as the Navier-Stokes (NS) equations. The term denotes the direct numerical solution of the equations (DNS) as well as more approximated solutions that are computationally less expensive, such as large-eddy simulations (LES) and Reynolds-averaged Navier-Stokes (RANS) [24].

Wind turbines have proven hard to treat in CFD due to the wide range of length scales involved in their aerodynamic behavior. The use of Reynolds-averaged Navier-Stokes (RANS) allows to save computational time, but can not model unsteady behaviour. Since the introduction of the actuator line approach (ALM) by Sørensen and Shen in 2002 [28], the use of LES for wind turbines has gained popularity in research ([17, 8]). The approach consists in modeling the turbine blades as discrete points at every blade element that exercise forces on the fluid. While the approach is computationally much more expensive than engineering models such as BEM, LES results can be obtained at a reasonable computational cost and find increased application as benchmark solutions for the verifications of simplified models. In the present work, this is attempted for a newly developed wake modeling tool. The LES library YALES2, developed originally 2003 by V. Moureau and maintained principally by the CORIA laboratory n Rouen [25], is used for. ALM capabilities were added only recently to this solver [8], and difficulties in the process are expected.

3. Implementation of a DWM-based wake modeling tool

A complete wake modeling tool according to the standard IEC4100 was implemented. The tool is able to deal with wake superposition in arbitrary farm layouts and can generate wind input data for an aero-servo-elastic solver. While the approach is standardized, many choices were left to be made during the implementation. The details of this implementation are outlined.

3.1. Wake Deficit

The wake deficit model is a refined Ainslie-type model as proposed by the standard [21, 15]. The model is formulated in non-dimensional variables with respect to the unperturbed wind speed and rotor diameter respectively. For the numerical schemes, a 4th-order finite difference scheme is chosen for the radial derivatives, while 1st-order backwards differences are used for axial derivatives [10]. The corresponding stencil is shown in figure 3. The choice of using backwards differ-

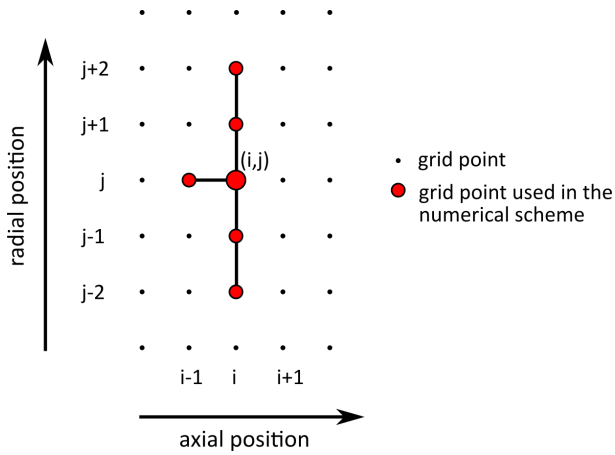

Figure 3: Points involved in the discretization of the continuity and momentum equation at the point (i, j)

ences is convenient, as it allows to directly propagate the solution in axial direction from the inlet boundary. For each axial advancement, an iterative approach is applied:

- Values for axial velocity at the new axial position are initialized to the values from the previous axial position
- Values for radial velocity at the position are computed directly from the discretized mass conservation equation
- Momentum balance is used to find a correction for axial velocity at all points
- The procedure is iterated until the largest velocity corrections falls below 10^{-3}

The boundary conditions are crucial to the correct solution of the problem. The inlet boundary condition is defined by the local axial induction factor $a(r)$ at each rotor section, pre-calculated by a BEM model for a range of velocities. Since the employed Ainslie-type deficit model neglects the pressure term in the NS equations, it cannot simulate the wake expansion in the near wake that is characterized by pressure equilibration. The approach suggested instead is to assume that the velocity reaches the far-wake value predicted by momentum theory,

$$U = U_0(1 - 2a), \tag{4}$$

immediately after the rotor. Initial wake expansion is taken into consideration as suggested in the standard. This approach leads to a non-physical result in the region immediately behind the rotor, as can be seen in a comparison with LES results for the same case (figure 4).

For lateral boundary conditions, it was chosen to impose ambient velocity at a distance of 4 rotor diameters from the centerline. In order to avoid

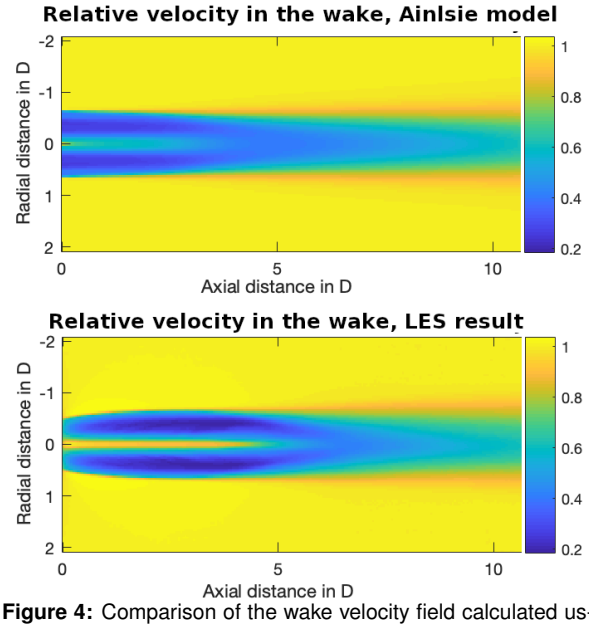

Figure 4: Comparison of the wake velocity field calculated using the DWM wake deficit model and LES, showing the difference in wake shape in the immediate near wake region.

the use of a Neumann (zero gradient) boundary condition at the center, the domain was mirrored along the rotor axis, sacrificing performance for a simpler implementation. The momentum added to the flow by the Dirichlet boundary conditions is negligible due to the large domain size. Added turbulence was implemented strictly according to the IEC standard. For wake meandering the suggested filter was implement using an infinite impulse response (IIR) first order digital filter [18]. The base signal for filtering is retrieved from the velocity time series at the rotor center, derived from turbulent inflow data. In order to compute the wakes of turbines that are themselves impacted by a wake, it is necessary to define a formulation used to compute the average wind speed and turbulence intensity, as these are the inputs of the DWM tool. Meandering necessarily has an effect on these average value, and needs to be considered both for velocity and turbulence. A process for this averaging is proposed:

1. The target turbine is discretized by a number of P points with corresponding numerical quadrature weights w_p.
2. The meandering offset time series for an impacting wake at the location of the target turbine is computed, resulting in T offset values in lateral and vertical direction.
3. For each quadrature point p and each meandering time step t, the location of p relative to the incoming meandered wake is computed.
4. For the $P \times T$ resulting points, the wake

deficit is computed through interpolation of pre-calculated results from the wake deficit model, yielding a velocity deficit time series of the length of the offset time series for each point p.

5. The deficit at each quadrature point p is time averaged, and by using the quadrature weights w_p the average velocity deficit across the rotor is computed.

6. The process is repeated for all N wakes that impact the target turbine, adding the mean deficits under the assumption of linear wake superposition

Using a nomenclature where $\Delta U(n,p,t)$ denotes the deficit caused by turbine n at the location p at the time step t, the procedure described above can be summarized in the following equation:

$$\langle \Delta U \rangle = \sum_{n=1}^{N} \sum_{p=1}^{P} \frac{\sum_{t=1}^{T} \Delta U(n,p,t)}{T} w_p, \tag{5}$$

and when wind field shear is considered as well, the equation for the average wind speed across the impacted rotor becomes:

$$U_w = \sum_{p=1}^{P} U_{shear}(p) w_p - \langle \Delta U \rangle. \tag{6}$$

A similar, but more elaborate process is repeated for the average turbulence, and average variance σ_{tot}^2 computed in 3 steps as follows:

$$\langle \sigma_{wm}^2 \rangle = \sum_{n=1}^{N} \sum_{p=1}^{P} \frac{\sum_{t=1}^{T} \left(\Delta U(n,p,t) - \langle \Delta U(n,p) \rangle_T \right)^2}{T} w_p, \tag{7a}$$

$$\langle \sigma_{wt}^2 \rangle = \sum_{n=1}^{N} \sum_{p=1}^{P} \frac{\sum_{t=1}^{T} k_{wt}^2}{T} w_p, \tag{7b}$$

$$\langle \sigma_{tot}^2 \rangle = \langle \sigma_{wm}^2 \rangle + \langle \sigma_{wt}^2 \rangle + \sigma_{amb}^2. \tag{7c}$$

The averaging approaches presented here are original to this work, as no documentation or literature on a similar averaging procedure is found.

In order to generate input for an aero-servo-elastic solver of choice, an already existing mechanism to input turbulence into the solver is used: *turbulence boxes*. These files describe the turbulent velocity component of a 3D wind field discretized on a box of a certain size and resolution depending on the diameter of the target turbine. The height and width of the box contain the full rotor disk, while the length is such that running through the box at mean ambient wind speed takes al long as the simulation. During the simulation, this box is moved across the rotor at ambient mean wind speed to deduce turbulent velocity at each blade element. By adding the wake effects computed by the implemented tool onto these boxes, as sown in figure 5, they can be applied directly to the aero-servo-elastic simulation without requiring any modifications to the solver.

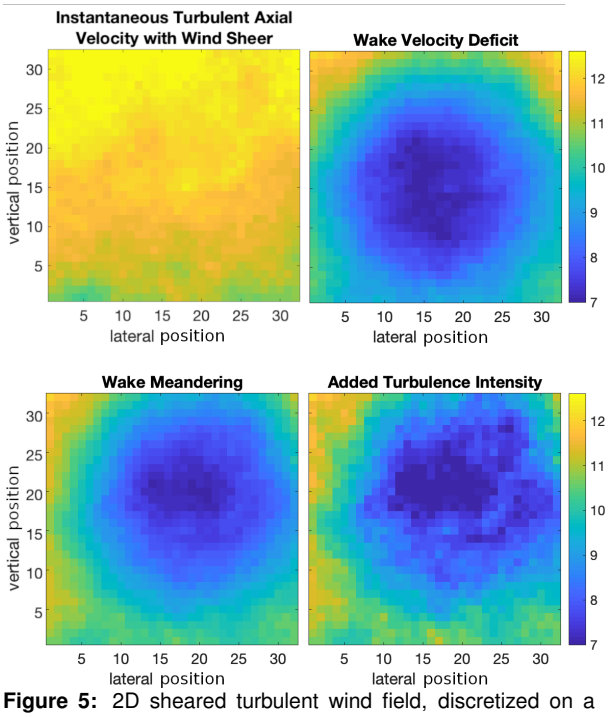

Figure 5: 2D sheared turbulent wind field, discretized on a 32x32 grid, successively showing the impacts of added wake effects.

The implemented wake modeling tool is a complete interpretation of an advanced engineering models for wakes, and the interface with the aero-servo-elastic solver allows for a precise evaluation of wake loads on turbines. The tool inherits some limitations from the underlying models, such as the approximation of an antisymmetric wake, the non-pysical results on the near-wake and the unrealistic assumption of constant meandering velocity even for very high distances.

4. Validation and Verification

A validation and verification of the implemented wake modeling tool is carried out. Initial verification focuses on the Ainslie wake deficit model as doubts emerged about its ability to conserve mass and momentum. Validation is carried out with field data for a turbine impacted by single wake. A additional verification is performed by benchmarking the tool with a solution generated from LES

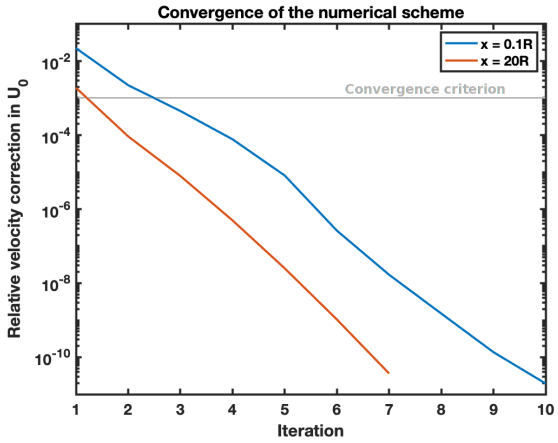

Figure 6: Convergence of the numerical scheme for a point in the near wake and a point in the far wake, showing the velocity correction obtained by solving equation **??**. The chosen convergence criterion is indicated.

4.1. Verification of the Ainslie Model

In order to asses the correctness of the implemented axisymmetric thin sheer layer Navier-Stokes flow solver, convergence and conservativeness are analysed.

Excellent results are found for convergence and are shown in figure **??**. The velocity correction decreases by one order of magnitude per iteration step over a wide range.

Conservativeness is asses by computing mass and momentum flow over a cylinder of radius 4 diameters, based at the rotor center and growing. Figure 7 shows the mass and momentum flow imbalance over such cylindrical control volumes for a wide range of velocities. It is important to note that at no point the relative imbalance in mass or momentum exceeds 1%. Verification of the implemented Ainslie model is therefore considered successful.

For validation of the model with field data, measurement results for wind speed and turbulence at various wind conditions were provided by the industrial partner. Data is available as 10 min statistics. The quantities are not retrieved from direct measurements, but rather estimated: wind velocity is deducted from power curves, while wind fluctuation, *i.e.* turbulence, is estimated from the fluctuations on measured loads. For the validation, the farm has been reconstructed numerically in the tool, and the procedure described in the previous section was applied to obtain results for average velocity and turbulence intensity for a given wind direction. Results can be seen in figures 8 and 9.

The results show an overall good agreement between the model and measurements. The velocity predicted by the model is lower than the average of the measured data, especially at low wind speeds. This might indicate that the wake deficit is cali-

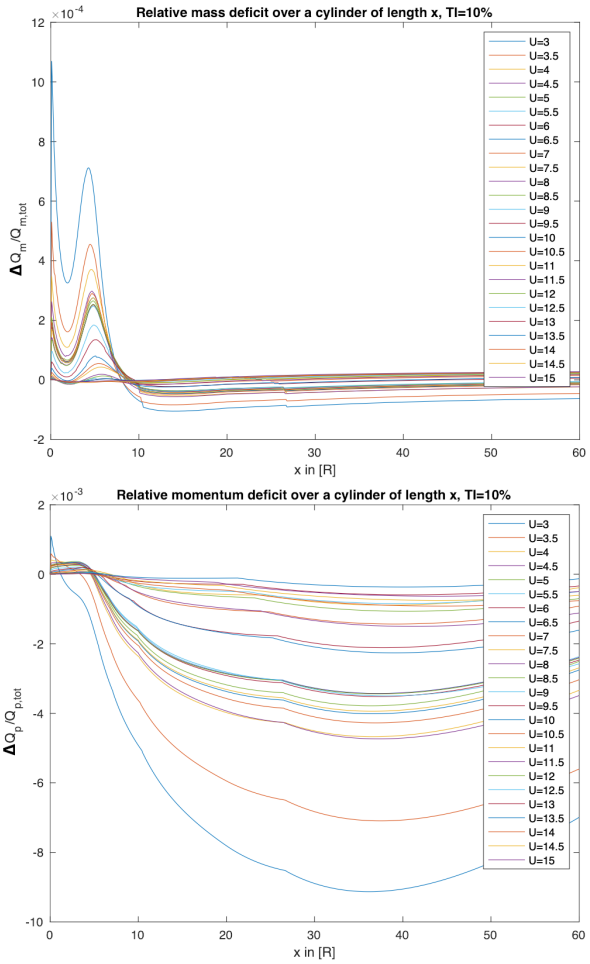

Figure 7: Relative mass and momentum flow deficit over a cylinder of Radius 4D and length x, normalized by the total flow over the inlet. Results for a range of relevant velocities.

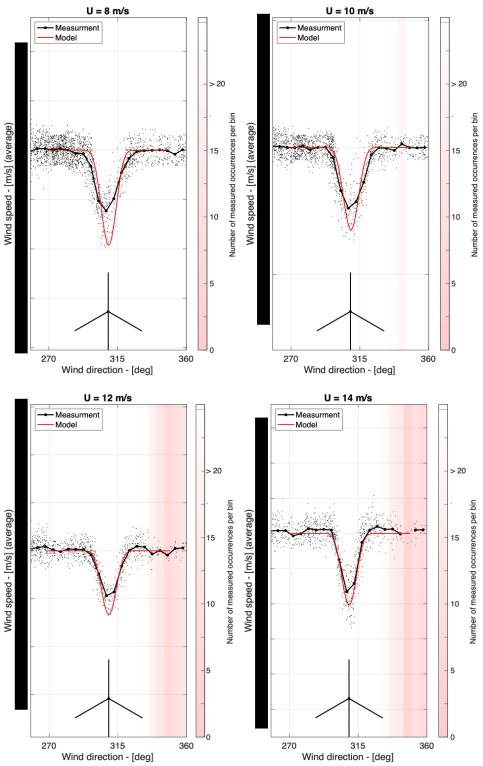

Figure 8: Comparison of the model results for average wind speed with data for different unperturbed wind speeds (1 m/s bins) at different inflow angles. Black dots represent average values over 5 degree bins. Model results have been obtained using the average undisturbed ambient turbulence. Pink shading indicates angular bins with limited data points.

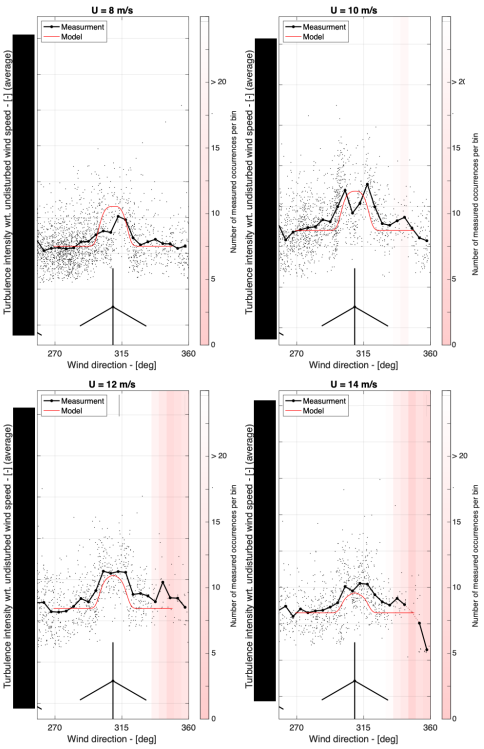

Figure 9: Comparison of the model results for turbulence with data for different unperturbed wind speeds (1 m/s bins) at different inflow angles. Black dots represent average values over 5 degree bins. Model results have been obtained using the average unperturbed ambient turbulence. Pink shading indicates angular bins with limited data points.

brated for around-rated wind speed, which makes sense as this is where the highest loads are expected to occur. On the other hand the computed turbulence is generally lower than what measurements show, especially at high wind speeds, and the base of the predicted ”bell shape” is too narrow. This seems to indicate a problem in the added turbulence model, since at high wind speeds (14 m/s) the velocity deficit, resulting from the deficit and meandering model, matches well with measurements. The experimental validation performed in the course of this work was limited in scope due to the nature of the data, notably lacking any validation of the predicted wake shape and velocity distribution across an impacted rotor. Furthermore, measurement data is available for local turbine loads from strain gages. Predicting these loads is one of the ultimate goals of this simulation tool. It is therefore of interest to use the tool to generate wind field input data for an aeroelastic solver, obtaining simulated results for loads to compare with measurements.

4.2. Verification with a High-Fidelity Flow Solver

Results of the implemented wake modeling tool are compared to LES results computed with the computational fluid dynamics library YALES2. The LES

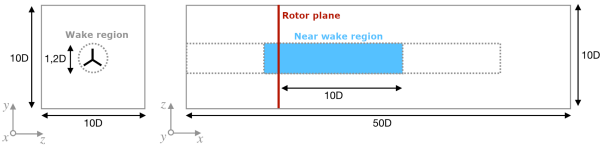

Figure 10: Simulation domain of the LES computation, with dimensions in turbine diameters D. The dotted outline denotes a region of local grid refinement, while in the blue area the grid is refined even further.

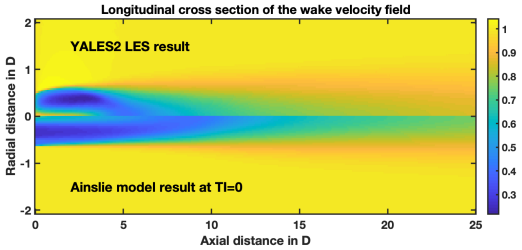

Figure 11: Comparison of the velocity field in the wake between the LES result (top) and the implemented wake deficit model (bottom) at 0% ambient turbulence

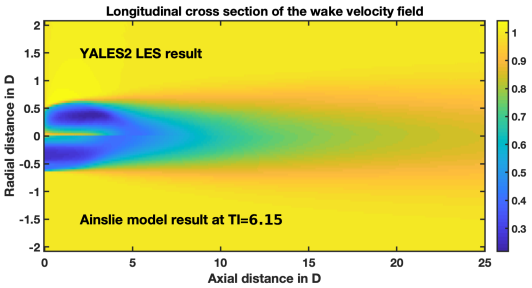

Figure 12: Comparison of the velocity field in the wake between the LES result (top) and the implemented wake deficit model (bottom) at the fitted ambient turbulence, 6.15%.

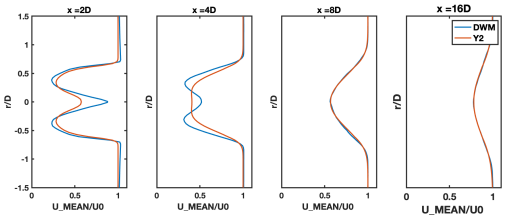

Figure 13: Comparison of the velocity profile in the wake at various downstream distances between the LES result and the implemented wake deficit model at the fitted ambient turbulence, 6.15%.

results were obtained n a 71.1 million cell unstructured grid, locally refined in regions of interest. The dimensions of the domain are shown in figure 10. Minimal random velocity fluctuations (1%) were injected after a grid study showed that this facilitated convergence. An initial flow field was computed on a 9 million element grid on the same domain, before acquiring statistics over 38 minutes of physical time, or approximately 350 rotor rotations. To compare to results of the tool, mean velocity was extracted from an axial cross section.

First comparisons were made by running the deficit model at 0% turbulence, but rather poor results were found, as can be seen in figire **??**. This is believed due to the model being miscalculated for cases of no ambient turbulence. It was therefore attempted to fit the model to the LES results by adapting the turbulence. At 6.15% turbulence, a near-perfect match between the tool and the LES solution was found, seen in figures **??** and 13. It can therefore be concluded that apart from one fitting parameter in the eddy viscosity model, the implemented Ainslie model matches well with an LES solution beyond a downstream distance of about 5-6 turbine diameters. It is however not advised to modify the parameters in the implementation in order to fit the available LES data. The case of 0% turbulence does not have any practical interest and the parameters recommended in the IEC standard for wind turbines have been validated more thoroughly. ¸

Several limitations of the LES model have been encountered during the verification. The lack of a way to inject turbulence at a desired intensity made a direct comparison impossible. The lack of a blade deformation model in LES made it necessary to use the polars of a deformed blade, that theoretically have to be generated for every operating condition. And lastly, the computational cost was substantial, with the generation of the benchmark consuming 12.079 processor hours and 500kWh of electricity. Running such computation for more than a hand full of validation cases is completely unfeasible.

5. A Novel Wake Steering Model Based on an Ainslie-Type Deficit Model

In the context of wind farm optimization, wake steering through yaw control is sliding into the focus of academic and industrial research alike [14]. Numerical models for the phenomenon of yaw deflection are necessary to validate the effectiveness of such control strategies. The first such model was proposed by Jiménez in 2010, and is based on lateral momentum conservation assuming a Jensen-type, top-hat shaped wake deficit [17]. The Jiménez model has been shown to overestimate wake deflection [7], and several new formulations have been proposed since then [7, 26]. In the following section, a semi-analytical wake deflection model for yawed turbines is derived. Conceptually, the model is similar to the Jiménez model as it is based on a lateral momentum balance, but also borrows elements from the deflection model of Bastankhah & Porté-Agel [**?**] that is based on a Gaussian deficit model. In contrast to other models found literature, the newly proposed model however does not make an assumptions on the wake shape, but rather uses the result form the Ainslie wake deficit model proposed in the DWM model

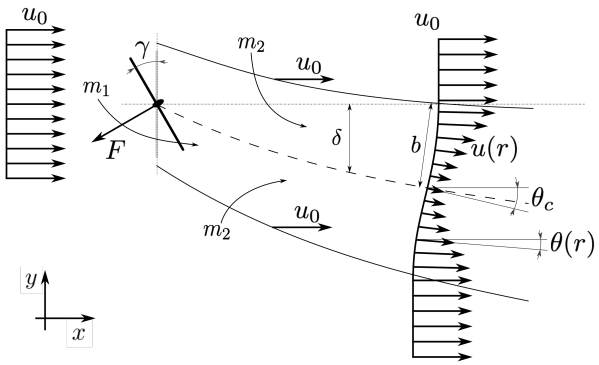

Figure 14: Schematic representation of the proposed wake steering model based on an Ainslie-type wake deficit model. The velocity in the wake $u(r)$ is taken from the deficit model at a given downstream distance, while the central deflection angle θ_c is retrieved from a momentum balance over the wake stream tube.

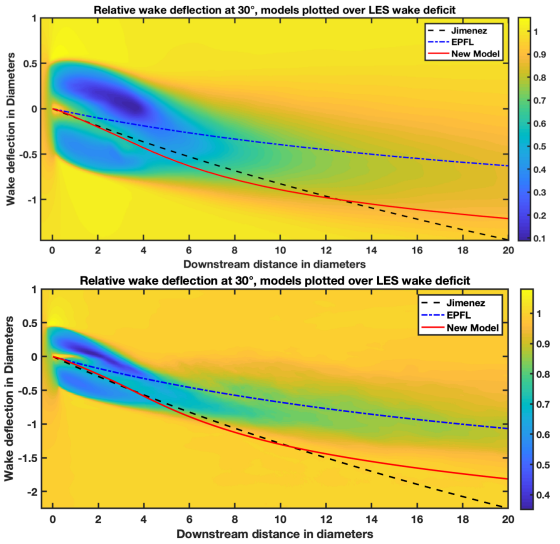

Figure 15: Comparison of the wake deflection models from literature and the new deflection model. Centerline deflection plotted on top of results from an LES-ALM simulation. Cases at 15 and 30 degree yaw misalignment.

[**?**, 21, 15]. This eliminates the need for additional parametrization beyond what is needed for the DWM model.

5.1. Derivation of the model

A derivation of the model follows. For the deflected stream tube, schematically shown in figure **??**, the following momentum balances can be written:

$$\vec{F} = \vec{Q}_{p,3} - Q_{m,1}\vec{u_0} - Q_{m,2}\vec{u_0}. \tag{8}$$

In this equation $\vec{Q}_{p,3}$ denotes the momentum flux over the outlet of the stream F tube, $Q_{m,1}$ is the mass flux over the domain inlet, $Q_{m,2}$ the entrained mass flux and $\vec{F}$ the total body force excreted by the wind turbine on the flow, deduced from the turbine local axial induction computed by BEM. The momentum balance is projected in axial and lateral direction, leading to the following of equations:

$$F\cos\gamma = Q_{p,3,x} - Q_{m,1}u_0 + Q_{m,2}u_0 \tag{9a}$$

$$F\sin\gamma = Q_{p,3,y} \tag{9b}$$

A last assumption is made: The wake skew angle $\theta(r)$ is assumed to follow the same distribution as the velocity deficit according to the expression:

$$\theta(r) = \theta_c \frac{\Delta u(r)}{\Delta u_c} \tag{10}$$

where θ_c and Δu_c are the centerline wake deflection angle and velocity deficit respectively. This assumption is similar to the one in Bastankhah et al. [6], where related Gaussian distributions for deficit and deflection angle are assumed. The assumption allows to derive a model based purely on the lateral momentum balance, and the final integral expression for the centerline deflection angle θ_c (under the assumption of small deflection angles) reads:

$$\theta_c \approx \frac{\cos^2\gamma \sin\gamma \int_0^R a(r)(1-a(r))rdr}{\int_0^b \left(1 - \frac{\Delta u(r)}{u_0}\right)^2 \frac{\Delta u(r)}{\Delta u_c} rdr} \tag{11}$$

Integrating the tangent of θ_c numerically along x finally gives the deflection δ of the wake centerline at any given downstream distance. All integrations have to be performed numerically, as the information on $\Delta u(r)$ is available only in discrete points from the Ainslie deficit model.

5.2. Comparison to other models

Results of the newly developed approach are compared with models commonly employed in wind turbine research and industry, the model by Jiménez [17], the Gaussian model by Bastankhah and Porté-Agel [7] (parametrized according to recent work by Altun [5]) and finally a LES study performed using the numerical set-up described previously. Results of the comparison for cases of 15 and 30 degree yaw (figure 15) show that the new model performs relatively well, giving similar results to the Jiménez model, but outperforming it in the far wake (). A well-calibrated Gaussian model outperforms the novel formulation. Conclusions are drawn considering the LES result can be taken as a reference, but the results suffer from the same limitations that were encountered during the verification study of the wake modeling tool, meaning that the results do not represent a perfect reference.

6. Conclusion

A fully operational wind farm aerodynamic modeling tool based on the DWM approach was implemented successfully. The support of wind farms made it necessary to adapt choices that are not documented elsewhere in literature, notably introducing an original approach to averaging meandering wakes to obtain input parameters for the wake models at hither rank turbines. While the tool could not be extensively validated, the underlying flow solver was verified and first results of the tool are promising. After some additional validation work, in particular regarding the superposition and farm aspects, the implemented tool could become a valuable asset for wind farm design and load assessments. The successful use of YALES2 in the verification of wind turbine wake models was demonstrated, even though some issues remain to be resolved before the benchmark solution generated by the LES solver can be fully trusted. Notably, a standard procedure for injecting and modeling ambient turbulence as well as for generating polars for given operating conditions should be proposed. Regarding the newly proposed wake deflection model, satisfactory result are found in a fist comparison, It is possible that the addition of more realistic turbulence in the LES model could change the comparison result. The novel approach assumes that the wake in yaw behaves the same as a regular wake and is simply shifted, but LES results suggest this is not the case. An improved parametrization of the Ainslie deficit model for yawed cases could lead to an improvement of this novel formulation.

References

[1] Global figures - offshore wind, September 2019.

[2] Openfast. `https://github.com/openfast`, August 2019.

[3] J. F. Ainslie. Wake modelling and the prediction of turbulence properties. *Proceedings of the Eighth British Wind energy Association Conference, Cambridge, Mar*, pages 19–21, 1986.

[4] J. F. Ainslie. Calculating the flowfield in the wake of wind turbines. *Journal of Wind Engineering and Industrial Aerodynamics*, 27(1-3):213–224, 1988.

[5] S. B. Altun. Modeling the effects of yaw-based wake steering on the downstream and crosswind neighboring wind turbines. Master's thesis, DTU, 3 2019. Master Thesis.

[6] M. Bastankhah and F. Porté-Agel. A new analytical model for wind-turbine wakes. *Renewable Energy*, 70:116–123, 2014.

[7] M. Bastankhah and F. Porté-Agel. Experimental and theoretical study of wind turbine wakes in yawed conditions. *Journal of Fluid Mechanics*, 806:506–541, 2016.

[8] P. Benard, A. Viré, V. Moureau, G. Lartigue, L. Beaudet, P. Deglaire, and L. Bricteux. Large-eddy simulation of wind turbines wakes including geometrical effects. *Computers & Fluids*, 173:133–139, 2018.

[9] E. Branlard. *Wind turbine aerodynamics and vorticity-based methods*. Springer, 2017.

[10] B. Fornberg. Generation of finite difference formulas on arbitrarily spaced grids. *Mathematics of computation*, 51(184):699–706, 1988.

[11] S. Frandsen. On the wind speed reduction in the center of large clusters of wind turbines. *Journal of Wind Engineering and Industrial Aerodynamics*, 39(1-3):251–265, 1992.

[12] S. T. Frandsen. *Turbulence and turbulence-generated structural loading in wind turbine clusters*. Risø National Laboratory, 2007.

[13] M. Gaumond, P.-E. Réthoré, A. Bechmann, S. Ott, G. C. Larsen, A. P. Diaz, and K. S. Hansen. Benchmarking of wind turbine wake models in large offshore windfarms. In *The science of Making Torque from Wind 2012: 4th scientific conference*, 2012.

[14] M. F. Howland, S. K. Lele, and J. O. Dabiri. Wind farm power optimization through wake steering. *Proceedings of the National Academy of Sciences*, 116(29):14495–14500, 2019.

[15] IEC TC 88. Wind energy generation systems - part 1: Design requirements. Technical Report IEC 61400, The International Electrotechnical Commission, Denmark, 2018.

[16] N. Jensen. A note on wind turbine interaction. *Risø National Laboratory, Roskilde, Denmark, Technical Report No. M-2411*, 1983.

[17] Á. Jiménez, A. Crespo, and E. Migoya. Application of a les technique to characterize the wake deflection of a wind turbine in yaw. *Wind energy*, 13(6):559–572, 2010.

[18] M. Klein, A. Sadiki, and J. Janicka. A digital filter based generation of inflow data for

spatially developing direct numerical or large eddy simulations. *Journal of computational Physics*, 186(2):652–665, 2003.

[19] G. C. Larsen. A simple stationary semi-analytical wake model. 2009.

[20] G. C. Larsen et al. Dynamic wake meandering modeling. 2007.

[21] H. A. Madsen, G. C. Larsen, T. J. Larsen, N. Troldborg, and R. Mikkelsen. Calibration and validation of the dynamic wake meandering model for implementation in an aeroelastic code. *Journal of Solar Energy Engineering*, 132(4):041014, 2010.

[22] H. A. Madsen, G. C. Larsen, and K. Thomsen. Wake flow characteristics in low ambient turbulence conditions. *Proceedings of the Copenhagen Offshore Wind*, 2005.

[23] J. F. Manwell, J. G. McGowan, and A. L. Rogers. *Wind energy explained: theory, design and application*. John Wiley & Sons, 2010.

[24] F. Moukalled, L. Mangani, M. Darwish, et al. *The finite volume method in computational fluid dynamics*. Springer, 2016.

[25] V. Moureau, P. Domingo, and L. Vervisch. Design of a massively parallel cfd code for complex geometries. *Comptes Rendus Mécanique*, 339(2-3):141–148, 2011.

[26] G.-W. Qian and T. Ishihara. A new analytical wake model for yawed wind turbines. *Energies*, 11(3):665, 2018.

[27] L. Savenije, T. Ashuri, G. Bussel, and J. Staerdahl. Dynamic modeling of a spar-type floating offshore wind turbine. In *Scientific Proceedings European Wind Energy Conference & Exhibition*, 2010.

[28] J. N. Sørensen and W. Z. Shen. Numerical modeling of wind turbine wakes. *Journal of fluids engineering*, 124(2):393–399, 2002.